Bose condensates at high angular momenta

S. Viefers,[1,3] T. H. Hansson,[2] and S. M. Reimann[1]
[1]*Department of Physics, University of Jyväskylä, Box 35, FIN-40351 Jyväskylä, Finland*
[2]*Department of Physics, University of Stockholm, Box 6730, S-11385 Stockholm, Sweden*
[3]*NORDITA, Blegdamsvej 17, DK-2100 Copenhagen, Denmark*
(Received 6 March 2000; published 16 October 2000)

We exploit the analogy with the quantum Hall (QH) system to study weakly interacting bosons in a harmonic trap. For a δ-function interaction potential the ''yrast'' states with $L \geqslant N(N-1)$ are degenerate, and we show how this can be understood in terms of Haldane exclusion statistics. We present spectra for four and eight particles obtained by numerical and algebraic methods, and demonstrate how a more general hard-core potential lifts the degeneracies on the yrast line. The exact wave functions for $N=4$ are compared with trial states constructed from composite fermions (CF), and the possibility of using CF states to study the low L region at high N is discussed.

PACS number(s): 03.75.Fi, 05.30.Jp, 73.40.Hm

The close relation between high angular momentum states of a condensate of *weakly* interacting hard core bosons [1–3] and the quantum Hall (QH) effect was recently pointed out [4–6]. The essential observation is that the weak interaction limit allows for a two-dimensional description of the boson system in terms of lowest Landau level (LLL) wave functions [4], just as for a QH system, and they are both described by wave functions containing powers of the Laughlin-Jastrow factor $\Pi_{i<j}(z_i - z_j)$, where z_i is the complex coordinate of the ith particle. As pointed out by Cooper and Wilkin [6], the two systems can in fact be mapped onto each other by a standard Leinaas-Myrheim transformation [7], attaching an odd number of units of statistical flux to each particle.

This enables us to use both intuition and techniques from the QH system to study rotating Bose condensates. In this paper, we shall mainly discuss the angular momentum region $N(N-1) \leqslant L \leqslant 2N(N-1)$, where the ground state corresponding to a δ-function two-body interaction is degenerate. We explicitly show how these degeneracies can be understood via a mapping to a system of free anyons in the LLL, and then show how the degeneracy is broken by a more general short-range potential containing derivatives of delta functions. We also make a detailed comparison between algebraically calculated exact wave functions and trial wave functions formed from so-called compact states of composite fermions, a construction orginally due to Jain and Kawamura [8]. In particular, we will emphasize the importance of a certain class of wave functions where the polynomial part is translationally invariant.

Although for computational reasons we have results only for few particles, $N=4$, 6, and 8, it is clear that some of our results, like the degeneracy structure of the yrast line, hold for any N. We also believe that many features of the results for the CF wave functions will generalize to higher N.

Since the flux attachment changes the angular momentum by $mN(N-1)/2$, where m is the number of fluxes attached, the boson-fermion mapping would apparently only be useful for studying angular momenta that are out of reach of present experiments [9] (which are limited to the strong interaction regime and $L \sim N$). However, there are some indications that fermionic techniques could be useful for L as low as N, i.e., for the so-called single vortex state. Although we will return to this point at the end of the paper, we shall for now, without any further apologies, consider the theoretical problem of understanding the region $N(N-1) \leqslant L \leqslant 2N(N-1)$ of the yrast line.

The simplest model for a hard-core interaction is a delta function potential. We thus consider a model of N interacting spinless bosons in a harmonic trap of strength ω. In the limit of weak interaction, this may be rewritten [4] as a two-dimensional lowest Landau level (LLL) problem in the effective ''magnetic'' field $B_{eff} = 2m\omega$ with the Hamiltonian taking the form

$$H = \omega L + g \sum_{i<j} \delta^2(\mathbf{r}_i - \mathbf{r}_j) \tag{1}$$

($\hbar = 1$), where $L \equiv \Sigma_i l_i = L_z$ is the total angular momentum. The single-particle states spanning our Hilbert space are $\eta_{0,l} = (2^{l+1}\pi l!)^{-1/2} z^l \exp(-\overline{z}z/4)$ with $z = \sqrt{2m\omega}(x+iy)$.

In Figs. 1 and 2 we show the interaction energy, in units of $g/4\pi$ as a function of the total angular momentum L for $N=4$, $L \leqslant 20$, and $N=8$, $30 \leqslant L \leqslant 56$, respectively. The many-body states are obtained from Lanczos diagonalization suitable for large and relatively sparse matrices [10]. The Fock space is spanned by single-particle states that are characterized only by the positive quantum numbers l, where $0 \leqslant l \leqslant L$. (Similar exact diagonalization studies have recently been reported in [6] and [11].) We note the following properties in the many-body spectra: Since increasing the angular momentum spreads out the particles in space, the yrast energy, i.e., the lowest possible interaction energy for given L, decreases with increasing L. For each state in the spectrum, there exists a set of ''daughter states'' with higher values of L, having exactly the same (interaction) energy as the original state. These daughters are simply center-of-mass excitations of the original states, thus having the same many-body correlations [12].

For $L \geqslant N(N-1)$ there are zero energy states, which can be understood by noting that any wave function of the form

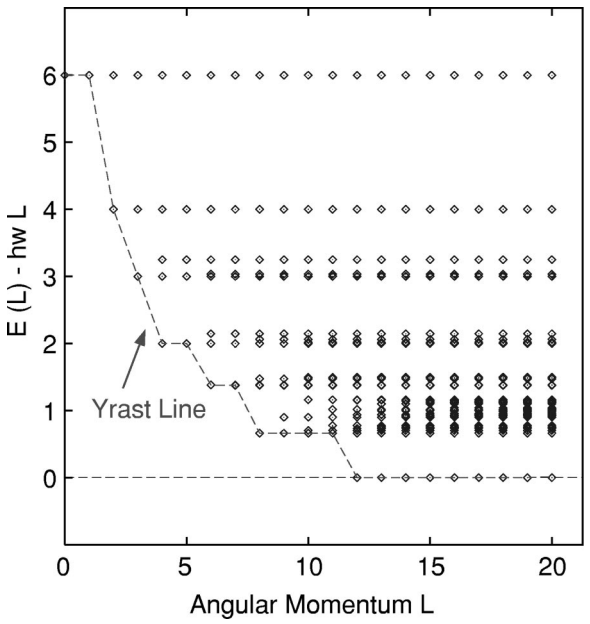

FIG. 1. Many-body spectra of $N=4$ weakly interacting bosons in a harmonic trap for $L\leqslant 20$. The dashed line connects the yrast states

$$\psi(z_1,z_2,\ldots,z_N)=\prod_{i<j}(z_i-z_j)^2 S(z_1,z_2,\ldots,z_N), \quad (2)$$

where $S(z_1,z_2,\ldots,z_N)$ is a symmetric polynomial in the z_i's, has zero interaction energy. Since the factor $\Pi_{i<j}(z_i-z_j)^2$ contributes an angular momentum $L_0=N(N-1)$, states of the type (2) exist for $L\geqslant L_0$.

At $L=N(N-1)$ there is a unique state with zero interaction energy corresponding to $S(z_1,z_2,\ldots,z_N)=1$, while the states at higher L typically are degenerate. The systematics of these degeneracies can be understood by a mapping to anyons in the lowest Landau level. The essential observation is that the wave functions (2) describe anyons in the LLL with statistics parameter $\alpha=2$ [13] (in general, the statistics parameter is given by the exponent of the Jastrow factor). It

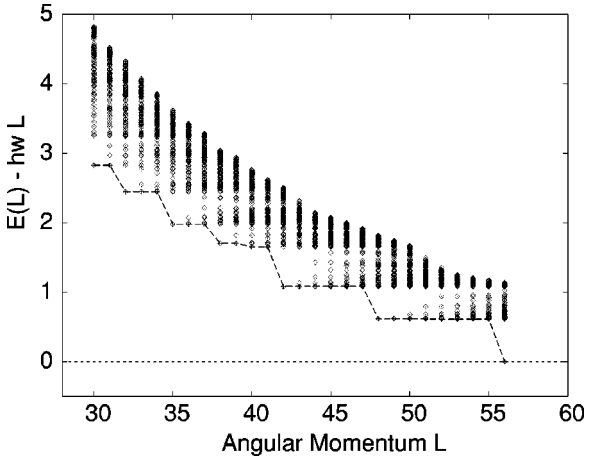

FIG. 2. As Fig. 1, but for $N=8$ and $30\leqslant L\leqslant 56$, showing only the 100 lowest eigenvalues

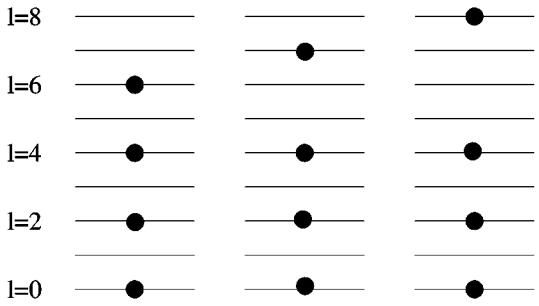

FIG. 3. FES construction of yrast states for $N=4$, $L=12(=L_0)$, 13, and 14. The $L=12$ and $L=13$ states are nondegenerate, whereas $L=14$ has degeneracy 2.

is known [13–15] that anyons in the LLL obey Haldane's fractional exclusion statistics (FES) [16], and following Ref. [13], one can use this knowledge to construct the allowed many-body states for given N and L as angular momentum excitations of the Laughlin-like state at $L=N(N-1)$. According to the definition of FES, each particle in the system blocks $\alpha=2$ single-particle states, and many-particle states with total angular momentum L are constructed by occupying single-particle states, with a minimum distance of $\alpha=2$ between each pair of occupied levels (for an example, see Fig. 3). The number of allowed configurations then gives the degeneracy of the state for a given L.

Table I shows the degeneracies of some of the states on the $N=4$ yrast line, as obtained from the anyon mapping, and they are in exact agreement with our numerical results.

This construction implicitly uses the fact that all the eigenstates on the yrast line for $L>N(N-1)$ contain the Jastrow factor $\Pi_{i<j}(z_i-z_j)^2$, so the degeneracies can also be found as the number of ways one can distribute $M=L-L_0$ units of angular momentum among N particles.

For a more general hard-core potential, the $E=0$ states on the yrast line above $L=N(N-1)$ are no longer degenerate. To demonstrate this point and study how the degeneracy is broken, we add a potential of the form

$$V=c_1\nabla^2\delta^2(z-z')+c_2\nabla^4\delta^2(z-z'), \quad (3)$$

that was originally used by Trugman and Kivelson [12] in the context of the fractional QH effect. The term $\sim\nabla^2\delta^2(z-z')$ does not contribute to the interaction energy for fully symmetric states, whereas the $\nabla^4\delta^2(z-z')$ term gives small corrections to the spectra in Figs. 1 and 2 [at the percent level for the parameters used in the inset of Fig. 4, where we show regularized forms of the potentials (1) and (3)].

We have examined how the potential (3) splits up the degeneracies of the zero interaction energy yrast states, by

TABLE I. Degeneracy d of the lowest L excitations above the Laughlin state for $N=4$.

L	12	13	14	15	16	17	18	19	20
d	1	1	2	3	5	6	9	11	15

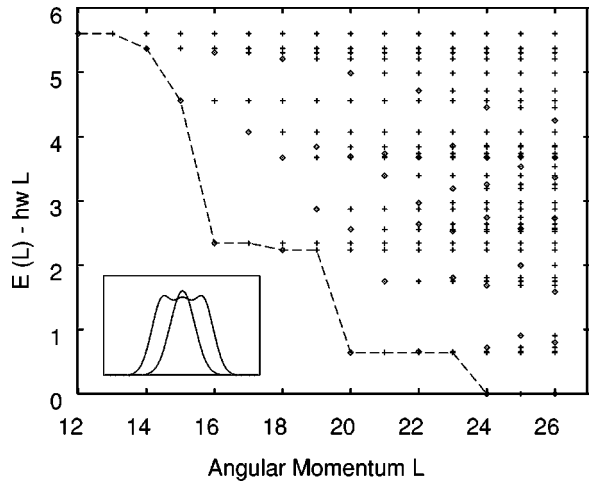

FIG. 4. Yrast spectrum for $N=4$ and $12\leqslant L\leqslant 26$, for a repulsive potential $\nabla^4\delta^2(z-z')$. Translation invariant eigenstates are denoted by diamonds, whereas the crosses denote center-of-mass excitations. Inset: Delta function potential (regularized as a Gaussian) and a potential including the terms (3), with $c_1=0.023$ and $c_2=0.000\,08$. We see that the latter more closely resembles a hard sphere potential.

exact algebraic diagonalization, using computer algebra. Here we have directly used the form (2), and systematically exploited that for a given L, all states corresponding to center-of-mass excitations of lower L-eigenstates are orthogonal to the subspace of ''new'' states. The latter subspace consists of translation invariant (TI) polynomials, i.e., functions invariant under a simultaneous, constant shift $z_i \rightarrow z_i+a$ of all the coordinates [12]. Following Trugman and Kivelson [12], we have used a basis constructed from elementary symmetric functions s_n. For given N and L, the basis consists of all possible combinations

$$|k_1k_2\cdots k_n\rangle \equiv s_1^{k_1}(z_i)s_2^{k_2}(\tilde{z}_i)\cdots s_N^{k_N}(\tilde{z}_N)\prod_{i<j}(z_i-z_j)^2, \tag{4}$$

such that $\Sigma_{n=1}^{N} nk_n = L-L_0$. Note that, for $n\geqslant 2$, we have introduced the new variables $\tilde{z}_i \equiv z_i - z_c$, with z_c the center-of-mass coordinate $z_c=(\Sigma z_i)/N$. The basis states spanning the TI subspace are identified as those with $k_1=0$. The diagonalization is thus performed within this subspace only, which reduces the matrix dimension substantially. The resulting spectrum for $N=4$, with the coefficient c_2 in Eq. (3) set equal to 1, is shown in Fig. 4.

We notice the close similarity between Figs. 1 and 4. In both cases, the yrast line passes through the same number of steps, with the same step lengths, as L is increased by $N(N-1)$, to the point where the yrast energy becomes zero. At the point $L=2N(N-1)$, the zero-energy yrast state is again nondegenerate and of the Laughlin type, i.e., $\Pi_{i<j}(z_i-z_j)^4$, whereas the subsequent yrast states have degeneracies corresponding to FES with statistics parameter $\alpha=4$. Including even higher derivative terms in the repulsive potential would subsequently split up the higher regions of the yrast line. Finally, note that the yrast states corresponding to cusps, i.e., states that are followed by a ''plateau'' in the yrast line, are always in the TI subspace.

The algebraic diagonalization used here is limited in practice to smaller particle numbers and angular momenta than the numerical scheme used in Figs. 1 and 2. However, the present approach has the advantage that it provides explicit, analytic expressions for the eigenfunctions, in terms of symmetric polynomials. This gives some additional insight into the structure of the yrast states, and in particular the region below the single vortex in the case of a pure delta function interaction. Bertsch and Papenbrock [11] recently proposed and numerically tested the following form for the yrast states at $2\leqslant L\leqslant N$,

$$\psi_L(z_i)=\sum_{p_1<p_2<\cdots<p_L}(z_{p_1}-z_c)(z_{p_2}-z_c)\cdots(z_{p_L}-z_c). \tag{5}$$

For the special case of the single vortex state $L=N$, this wave function was first proposed by Wilkin, Gunn, and Smith [4]. Eq. (5) is just the symmetric polynomial $s_L(\tilde{z}_i)$, i.e., the state $|0\ldots1\ldots0\rangle$ (with the 1 in the Lth place), in the notation of Eq. (4) (without the Jastrow factor in the present case of a pure delta function interaction). This state is a basis state in the TI subspace for all $2\leqslant L\leqslant N$. In the cases where this is the *only* basis state ($L=2,3$ for $N\geqslant 3$), it is thus obvious that Eq. (5) is exact. Furthermore, performing the algebraic diagonalization up to $L=N$ for $N=4$ and $N=6$, we have confirmed that even when the translation invariant subspace is spanned by more than one basis vector, the basis state (5) is always an exact eigenstate.

We now turn to a study of a class of wave functions that can be constructed in analogy with the so-called Jain states for the fractional quantum Hall effect [17]. The main idea is to map the strongly interacting LLL bosons to weakly interacting composite fermions by attaching an odd number m of flux quanta to each particle. Trial wave functions with angular momentum L are thus constructed as noninteracting fermionic wave functions with angular momentum $L-m/2N(N-1)$, multiplied by m Jastrow factors and projected onto the LLL,

$$\psi_L=\mathcal{P}\left(f_F(z_i,\bar{z_i})\prod_{i<j}(z_i-z_j)^m\right). \tag{6}$$

Here, f_F is a Slater determinant consisting of single-particle wave functions $\eta_{n,l}(z,\bar{z})\propto z^l L_n^l(\bar{z}z/2)$, where n is the Landau level index ($l\geqslant -n$), and L_n^l a generalized Laguerre polynomial.

Originally used for the homogeneous states relevant for the fractional QHE, wave functions of the type (6) were later employed to describe inhomogeneous systems such as quantum dots [8,18,19] and recently by Cooper and Wilkin [6] to study the bosonic yrast lines for up to 10 particles in the case of a pure delta function interaction.

In short, the LLL projection in Eq. (6) amounts to the replacement $\bar{z_i}\rightarrow 2\partial_i$ in the polynomial part of the wave function. However, there are several ways of doing this in

practice, and we shall compare the different projection methods when constructing trial wave functions for the yrast states in Figs. 1 and 4. The most straightforward way is to replace the $\bar{z}$'s with derivatives in the final polynomial, obtained after multiplying out the Slater determinant and the Jastrow factors and moving all $\bar{z}$'s to the left. In practice, this method is applicable only for small particle numbers, when the number of derivatives involved is not too large. We shall refer to this method as ''method I.''

Alternatively, noting that [17]

$$\begin{vmatrix} \eta_{11} & \eta_{12} & \cdots \\ \eta_{21} & \eta_{22} & \cdots \\ \vdots & \vdots & \vdots \\ \eta_{N1} & \eta_{N2} & \cdots \end{vmatrix} \prod_{i<j} (z_i - z_j)^{2p} = \begin{vmatrix} \tilde{\eta}_{11} & \tilde{\eta}_{12} & \cdots \\ \tilde{\eta}_{21} & \tilde{\eta}_{22} & \cdots \\ \vdots & \vdots & \vdots \\ \tilde{\eta}_{N1} & \tilde{\eta}_{N2} & \cdots \end{vmatrix}, \tag{7}$$

where $\eta_{ij} \equiv \eta_i(z_j, \bar{z_j})$ and $\tilde{\eta}_{ij} \equiv \eta_i(z_j, \bar{z_j}) \Pi_{k \neq j}(z_j - z_k)^p$, one can first absorb $2p$ Jastrow factors in the Slater determinant, and then project entry by entry. Since the wave function (6) contains an odd number m of Jastrow factors, one finally has to compensate by multiplying the resulting polynomial by $\Pi_{i<j}(z_i - z_j)^{m-2p}$. We shall refer to this as method II and use it as follows; for a delta function interaction, where the wave function contains $m=1$ Jastrow factor, it is appropriate to use $p=1$ (method IIa). Note that this means *dividing* the Slater determinant by one Jastrow factor. As the latter can be factorized from any fully antisymmetric polynomial, and we are using computer algebra for all manipulations, this poses no problem. In the case of the $\nabla^4\delta$-potential, the Jain construction will involve absorbing $m=3$ flux quanta in the wave function, and we shall compare projection with $p=1$ (method IIa) and $p=2$ (method IIb). [Note that method IIa is in a sense trivial, since it relates the wave functions at L and $L+N(N-1)$ by multiplication with two Jastrow factors.]

We have already stressed the significance of the TI subspace—these are the states that determine the shape of the yrast line. It is very appealing that there is a special set of the states (6) that are in this subspace, namely the so-called *compact states* [8] that are characterized by having the nth Landau level occupied from $l_n = -n$ to $l_n = l_n^{max}$ without any ''holes.'' In the context of the QH effect, the important property of the compact states is that they are homogeneous.

When describing quantum dots using the noninteracting composite fermion model (NICFM), one can show that CF candidates for the cusp states must be compact [8], and the same line of arguments was later used for bosons [18,6]. From the point of view of the wave functions, the importance of the compact states is that they are in the TI subspace, and it is rather remarkable that *for all L where a compact state can be constructed, the one with the lowest CF energy has a large overlap with the lowest exact state in the TI subspace.* This is true, independent of whether or not the state is a ground state, i.e., corresponds to a cusp in the yrast line. In the following discussion, we shall only be concerned with the wave functions, and will not discuss whether or not the NICFM can give a good description of the energy spectrum, a question that was already discussed in some detail [8,18,19].

TABLE II. Overlaps between trial and exact yrast wave functions for $N=4$, $0 \leqslant L \leqslant 12$ and a pure delta function interaction, using projection methods IIa and I (see text).

L	0	2	3	4	6	7	8	12
IIa	1	1	1	0.944	0.962	1	0.997	1
I	1	1	1	0.980	0.980	1	0.997	1

δ-function potential: In this case we have calculated the Jain wave functions (6) corresponding to all compact states for $N=4$, $0 \leqslant L \leqslant 12$, taking $m=1$ and using projection method IIa ($p=1$). If there are two compact states with the same L, we use the one with the lowest CF effective energy. In Table II, we show the overlap with the exact algebraic wave functions. A ''1'' indicates that the wave functions are identical. For comparison we have also included the overlaps with the wave functions corresponding to projection method I. (For some cases these were previously given by Cooper and Wilkin [6].) We note that *all* the compact states have very large overlap with the exact eigenstates. That the CF wave function is exact for $L=2,3$ is a simple consequence of the TI property and that there is only one state in the TI subspace at these L values. That the $L=7$ state comes out exact is more surprising, and we have no good explanation for this. It would be interesting to pursue the exact diagonalization to higher N in order to see if there are other nontrivial CF states that are exact. We also note that the direct projection (method I) does slightly better than method II.

$\nabla^4\delta$-function potential: Here we calculated the Jain wave functions (6) corresponding to all, lowest CF-energy, compact states for $N=4$, $12 \leqslant L \leqslant 24$ taking $m=3$ and using projection methods IIa ($p=1$) and IIb ($p=2$). For comparison, we also used method I. In Table III, we show the overlap with the exact algebraic wave functions. We again note that *all* the compact states (except $L=17$ with projection method I) have very large overlap with the exact eigenstates, and that for $L=17,19$, the CF state is not the ground state. Comparing the different projection methods, we see that in many, but not all cases they give identical results. In particular, one should note that methods I and IIb do not reproduce the exact wave function for $L=12,14,15$ where the TI subspace is

TABLE III. Overlaps between trial and exact yrast wave functions for $N=4$, $12 \leqslant L \leqslant 24$, using two different projection methods (see text). The asterisk indicates that the $L=17$ and $L=19$ Jain states (which correspond to the lowest TI states) are not yrast states, but lie higher in energy than the CM excitation of the previous L state. Note that projection method IIa gives zero for $L=17$.

L	12	14	15	16	17*	18	19*	20	24
IIa	1	1	1	0.988		0.910	0.993	0.986	1
IIb	0.938	0.910	0.988	0.990	1	0.910	0.993	0.986	1
I	0.993	0.970	0.998	0.990	0.591	0.906	0.993	0.986	1

nondegenerate. This means that these projections give wave functions that are not in the space of states given by Eq. (2). The same effect is even more striking for $L=17$, where method IIb gives the exact wave function, whereas direct projection (method I) gives a rather poor overlap, indicating that a large component is not in the subspace (2).

Finally, we briefly discuss the experimentally more relevant case of low angular momenta, $L\sim N$. In Ref. [5], Wilkin and Gunn used a composite *boson* (CB) approach to construct trial states with angular momenta $L=n(N-m)$ with n and m nonnegative integers. In particular, they found that the single-vortex CB state $(n=1,m=0)$ exactly reproduces the exact wave function (5). Here, we comment on the possibility to use CF wave functions for the single vortex state at $L=N$. Rather surprisingly, the overlaps between the CF and the exact wave function (5) tend to get *larger* with increasing particle number, at least up to $N=10$ [6]. It thus seems worthwhile to use the CF approach to construct trial wave functions for the single vortex for general N. The single vortex CF state is in fact unique, if one demands that in addition to being compact, it should also have minimal CF cyclotron energy. The relevant Slater determinant is formed from the single-particle states $\eta_{n,-n}$ for $n=N-2$, $N-1,\ldots,0$, and η_{01}, and, using projection method I, the resulting wave function takes the following rather compact form:

$$\psi_{L=N}=\sum_{n=1}^{N}(-1)^n z_n \prod_{k<l;k,l\neq n}(\partial_k-\partial_l)\prod_{i<j}(z_i-z_j). \quad (8)$$

As opposed to the CB wave function in Ref. [5], Eq. (8) is not exact, and we have not been able to calculate the overlap with the exact wave function for general N. Although the $\sim N^2$ derivatives make it difficult to evaluate this function for large N, it can easily be handled in integrals of the form $\int\Pi_i d^2z_i \exp(-1/2\Sigma_i \overline{z_i}z_i) f(\overline{z_i})\psi_{L=N}$ by partial integrations. Alternatively, one can use projection Method II, where the wave function becomes a determinant of linear combinations of elementary symmetric polynomials. In both cases, it should be possible to compare with the exact wave function (5) using Monte Carlo methods.

We are very grateful to B. Mottelson for introducing us to the physics of rotating Bose condensates, and for numerous fruitful discussions. We also wish to thank M. Manninen, G. Kavoulakis, and R. K. Bhaduri for discussions and M. Koskinen for giving advice on the numerical work. This work was financially supported by the Academy of Finland, the Swedish Natural Science Research Council, the TMR program of the European Community under Contract No. ERBFMBICT972405, the ''Bayerische Staatsministerium fur Wissenschaft, Forschung und Kunst,'' and the NORDITA Nordic project ''Confined electronic systems.''

[1] D. A. Butts and D. S. Rokhsar, Nature (London) **397**, 327 (1999).
[2] B. Mottelson, Phys. Rev. Lett. **83**, 2695 (1999).
[3] G. M. Kavoulakis, B. Mottelson, and C. J. Pethick, e-print cond-mat/0004307.
[4] N. K. Wilkin, J. M. F. Gunn, and R. A. Smith, Phys. Rev. Lett. **80**, 2265 (1998).
[5] N. K. Wilkin and J. M. F. Gunn, Phys. Rev. Lett. **84**, 6 (2000).
[6] N. R. Cooper and N. R. Wilkin, Phys. Rev. B **60**, R16 279 (1999).
[7] J. M. Leinaas and J. Myrheim, Nuovo Cimento Soc. Ital. Fis., B **37**, 1 (1977).
[8] J. K. Jain and T. Kawamura, Europhys. Lett. **29**, 321 (1995).
[9] M. R. Matthews *et al.*, Phys. Rev. Lett. **83**, 2498 (1999); K. W. Madison, F. Chevy, W. Wohlleben, and J. Dalibard, e-print cond-mat/9912015.
[10] R. B. Lehoucq, D. C. Sørensen, and Y. Yang, *ARPACK User's Guide: Solution to Large Scale Eigenvalue Problems with Implicitly Restarted Arnoldi Methods*. See http://www.caam.rice.edu/software/ARPACK
[11] G. F. Bertsch and T. Papenbrock, Phys. Rev. Lett. **83**, 5412 (1999).
[12] S. A. Trugman and S. Kivelson, Phys. Rev. B **31**, 5280 (1985).
[13] T. H. Hansson, J. M. Leinaas, and S. Viefers, Nucl. Phys. B: Field Theory Stat. Syst. **470**[FS], 291 (1996).
[14] S. B. Isakov and S. Viefers, Int. J. Mod. Phys. A **12**, 1895 (1997).
[15] A. Dasniéres de Veigy and S. Ouvry, Phys. Rev. Lett. **72**, 600 (1994); Y. S. Wu, *ibid.* **73**, 922 (1994); D. Li and S. Ouvry, Nucl. Phys. B **430**, 563 (1994).
[16] F. D. M. Haldane, Phys. Rev. Lett. **67**, 937 (1991).
[17] For a review, see J. K. Jain and R. K. Kamilla, in *Composite Fermions: A Unified View of the Quantum Hall Effect*, edited by O. Heinonen (World Scientific, River Edge, NJ, 1998).
[18] B. Rejaei, Phys. Rev. B **48**, 18 016 (1993).
[19] C. W. J. Beenakker and B. Rejaei, Physica B **189**, 147 (1993).